5-21-2004

The Synthesis of Core-Shell Iron@Gold Nanoparticles and Their Characterization

Zhihui Ban
University of New Orleans

THE SYNTHESIS OF CORE-SHELL IRON@GOLD NANOPARTICLES AND THEIR CHARACTERIZATION

A Thesis

Submitted to the Graduate Faculty of the
University of New Orleans
in partial fulfillment of the
requirements for the degree of

Master of Science
in
The Department of Chemistry

by

Zhihui Ban

B.S. Zhejiang University, P. R. China, 1996
Ph. D. Dalian Institute of Chemical Physics, P. R. China, 2001

May 2004

ACKNOWLEDGEMENTS

Many individuals have assisted me during graduate study, both at the Department of chemistry and at the Advanced Materials Research Institute where I was graciously allowed to perform my thesis research.

I would like to begin by thanking my major professor, Dr. Charles J. O'Connor for all of your guidance, assistance and support. I also thank my committee, Dr. John B. Wiley, Dr. Steven P. Nolan, Dr. Jiye Fang and Dr. Kevin Stokes, for your advice and encouragement.

I would like to thank Dr. Kevin Stokes and Dr. Yuri A. Barnakov for the Faraday rotation measurements and analysis, Dr. Vladimir O. Golub for the SQUID measurements and analysis.

I acknowledge the support from the Advanced Materials Research Institute through the Office of Naval Research Grant N00014-02-1-0729.

Special thanks to my wonderful wife, Yanjie, my parents and parents in law. Your love and support encourage me to go forward.

The thesis is also for my nine-month-old daughter, Angelina. You are my angel and the best gift for our family.

FOREWORD

“Advances in nanofabrication techniques are opening up a wide array of highly sophisticated biomedical applications for smaller and smarter magnetic particles. Areas under investigation include targeted drug delivery, ultra-sensitive disease detection, gene therapy, high throughput genetic screening, biochemical sensing, and rapid toxicity cleansing. Each of these disparate applications hinges on the apparently benign relationship between magnetic fields and biological systems; field strengths required to manipulate nanoparticles have no deleterious impact on biological tissue and the biotic environment does not shield efforts to detect internal magnetism. This makes magnetic nanoparticles highly attractive as in vivo probes or in vitro tools to extract information on biochemical systems.”

----------materialstoday February 2004

TABLE OF CONTENTS

LIST OF FIGURES

ABSTRACT

Au-coated magnetic Fe nanoparticles have been successfully synthesized by partial replacement reaction in a polar aprotic solvent with about 11 nm core of Fe and about 2.5 nm shell of Au.

In this work, a combination of TEM (transmission electron microscopy), XRD (X-ray Powder Diffractometry), EDS (Energy disperse X-ray spectroscopy), SQUID (Superconducting Quantum Interference Device), TGA (Thermograviometric analysis), UV-visible absorption spectroscopy and Faraday rotation were employed to characterize the morphology, structure, composition and magnetic properties of the products.

HRTEM images show clear core-shell structure with different crystal lattices from Fe and Au. SQUID magnetometry reveals that particle magnetic properties are not significantly affected by the overlayer of a moderately thick Au shell. The Au-coated particles exhibit a surface plasmon resonance peak that red-shifts from 520 to 680 nm. And all the above characterizations show that in this sample, there are no Fe oxides inside the particle.

CHAPTER 1 INTRODUCTION

Nowadays, magnetic nanoparticles are playing an important role in the wide range of sophisticated bio-medical applications, such as targeted drug delivery, biochemical sensing, and ultra-sensitive disease detection. The decrease of particle size leads to increase of its reactivity and their magnetic properties are dominated by superparamagnetism and surface effects [1]. Several works report a possibility to passivate a surface of magnetic nanoparticles (γ - Fe_2O_3, Co, Fe et al.) by another inert shell (SiO_2, gold, silver, polymer et al.)[2-9]. A diamagnetic layer could potentially reduce magnetic properties of the magnetic core of nanoparticle. Despite this, gold has become a favored coating material because of its specific surface functionality for subsequent treatment with chemical or bio-medical agents [10-11]. Meanwhile, it protects the magnetic core against oxidation, without drastic reduction of the magnetic properties. It is expected that iron nanoparticles can be passivated to avoid oxidation by gold coating and not modify the magnetic properties (such as coercivity or blocking temperature). The reverse micelle method for synthesis of Fe@Au nanoparticles has been previously

developed by our group [12]. In this work, we will present another simple method for the synthesis of gold-coated iron nanoparticles by partial replacement reaction. The idea of the method is to use reducing agents (Na, K, Li) to reduce ML_n (M = Fe, Co, Ni; L = Cl, Br; n = 2, 3) to form the metallic core nanoparticles[13], and then use the surface of metallic core particles to reduce Au^{3+} to form gold coated mettallic nanoparticles, as shown in scheme 1. Xia et al. [14] have used a similar concept with galvanic replacement reactions for generating metal nanostructures with hollow interiors.

CHAPTER 2 EXPERIMENT

The reduction reactions were conducted in polar aprotic solvents. In a typical synthesis, 2 mmol of $FeCl_3$ were dissolved in NMPO (1-Methyl-2-Pyrrolidinone) to form a yellow solution (# A). 6 mmol of Na were dissolved in NMPO with 6 mmol of naphthalene to form a dark green solution (# B). A 0.7 mmol of dehydrated $HAuCl_4$ was dissolved in NMPO (# C). The solution # A was added into solution # B quickly with intensive stirring at room temperature. The color of mixture changed to dark brown immediately. The mixture was further stirred for two hours and then centrifuged to remove the sodium chloride. Then a small amount of capping agent, 4-benzylpyridine, was added into the solution followed by heating and refluxing at 165°C for three hours. A black mixture was obtained and cooled to 60°C, and then solution # C was added slowly then heated with stirring to 125^{o}C for 4 hours. The product that was obtained was added to tetrahydronaphthalene and then centrifuged yielding a black paste which is the product. All the above synthesis operations were performed in an argon atmosphere glove box. The sample was dried in vacuum and washed with EtOH, 8% HCl solution, water

and EtOH several times until a colorless suspension was made. A further purification stage included a magnetic separation by magnetic field H = 5 kOe in order to get separate Fe@Au from pure gold nanoparticles. The magnetically separated powder was dried in the air and subjected to characterization by Transmission electron microscopy (TEM), Energy disperse X-ray spectroscopy (EDS), Superconducting Quantum Interference Device (SQUID), X-ray diffraction (XRD), Thermograviometric analysis (TGA), UV-visible absorption spectroscopy and Faraday rotation.

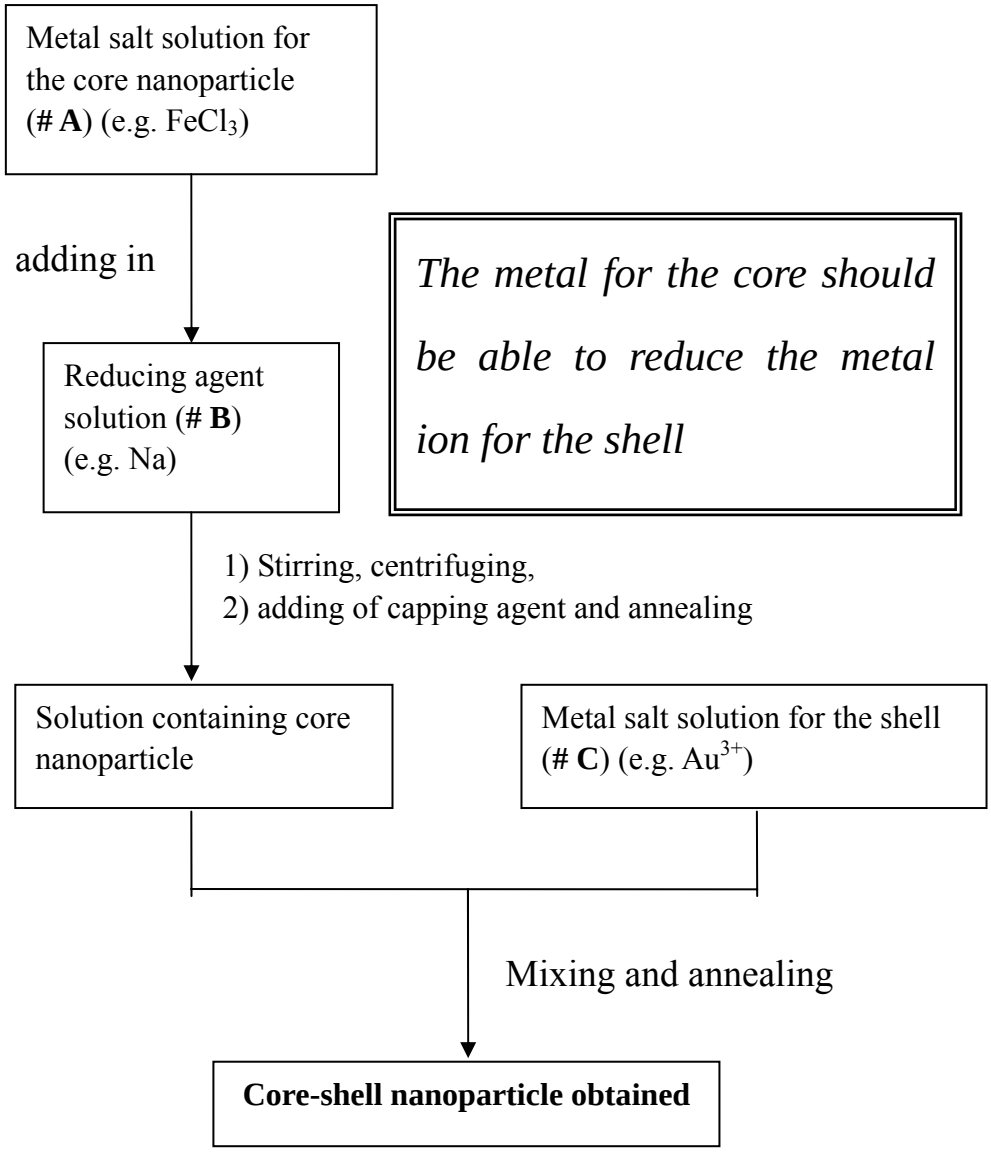

scheme 1. The reaction route to synthesize core-shell nanoparticles.

CHAPTER 3 RESULTS AND DISCUSSION

3.1 TEM characterizations

Figure 1(a, b, c) show three typical TEM images of gold coated iron nanoparticles. The dark contrast in the central part of the particles shows cores with a size of about 11 nm. The light contrast on the periphery of the particles shows the shells with a thickness of about 2.5 nm. The average diameter of the core-shell particle is 16 nm with ~15 % size deviation. The composition of the nanoparticles was estimated by EDS (Figure 1d). EDS shows the presence of copper, gold, and iron. The copper is from the TEM grid, and the gold and iron are from the sample. This result indicates that the molar ratio between Fe and Au is 1.4 : 1. The detailed core-shell structure (Fe@Au) of a single particle is observed in the high resolution TEM image in Figure 2. There are four representative HRTEM images. The crystalline Au shells are running directly from the surface of iron particle and have a different orientation from particle to particle. The lattice fringes of the shell are clearly shown with the spacing of ~2.4 Å and ~2.0 Å. This corresponds to the {111} and {200} lattice planes for gold, respectively. HRTEM images of our core-shell particles also

show crystal lattices of the iron core with interplanar distances ~2.0 Å and ~1.4 Å. This corresponds to the {110} and {200} lattice planes of iron, respectively.

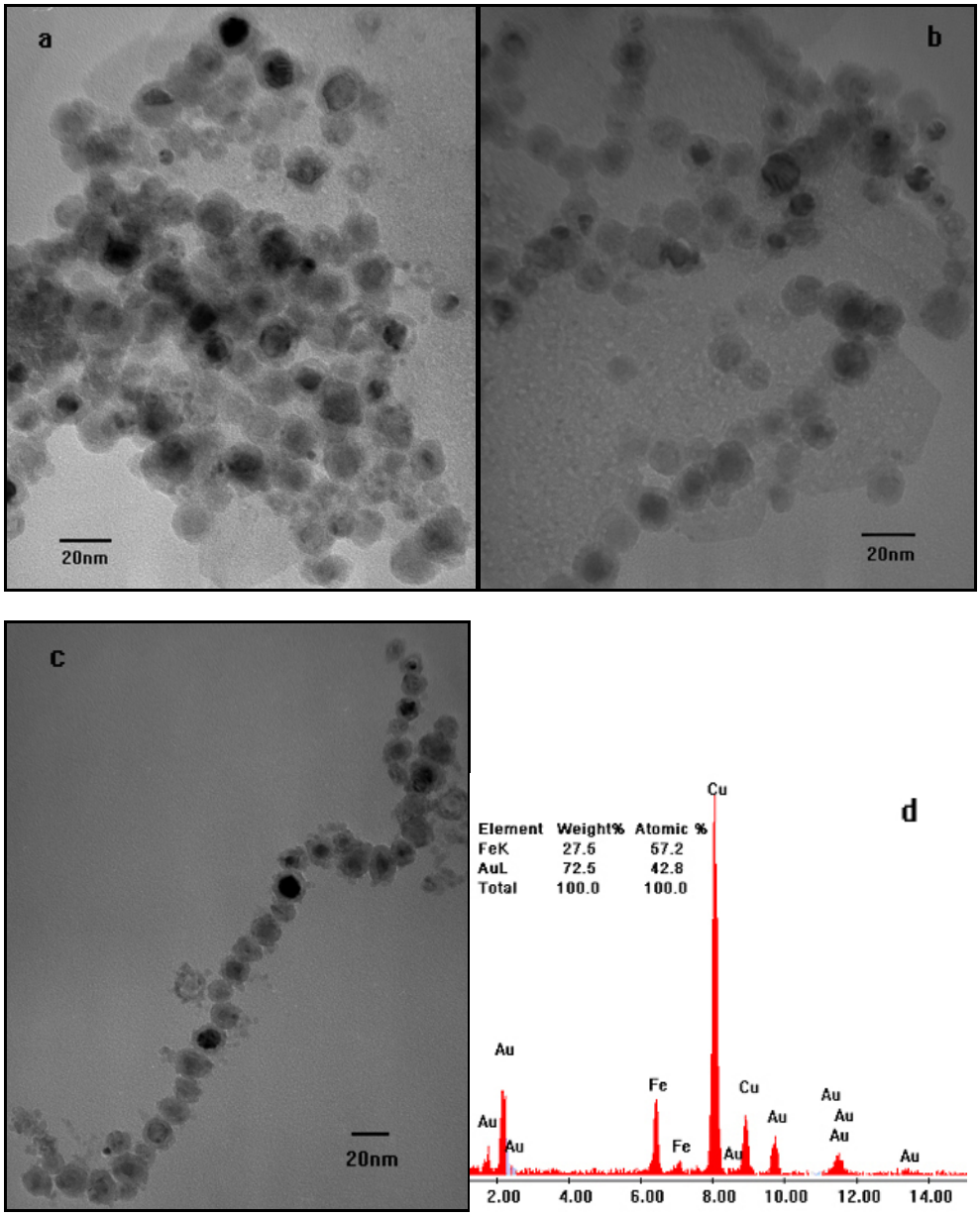

Figure 1. (a) (b) (c) TEM micrograph of iron coated with gold nanoparticle, about 16 nm. (d) EDS result of Fe@Au particle, the molar ratio Fe:Au = 57.2:42.8

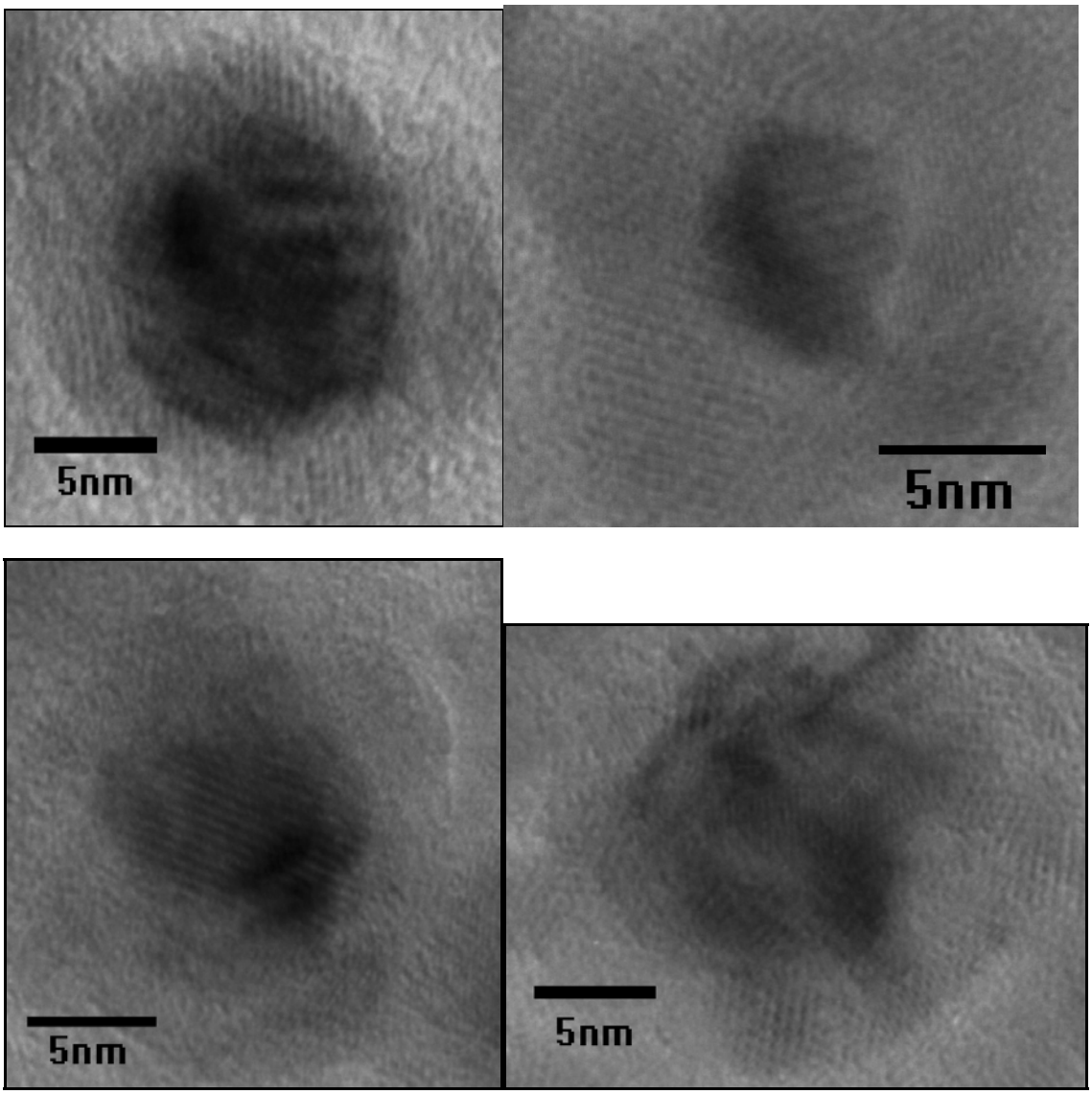

Figure 2. High-resolution TEM images of Fe@Au nanoparticles showing the fringes of (a) (111) and (b) (200) crystal planes of *gold* shells.

3.2 TGA characterization

The characterization of the core-shell structure of the sample can be studied by TGA measurements in different atmospheres. The TGA curves of the obtained sample in air (a) and 8% H_2 in argon (b) atmospheres are shown in Figure 3. From Figure 3a, one can only see the weight loss that is due to the decomposition of organic ligands in the sample. A similar TGA curve was obtained in hydrogen atmosphere (Figure 3b). There is also only weight loss. However, one can notice that, in the case of air atmosphere, the weight loss is a little bit smaller than it is in hydrogen. This difference is probably due to the fact that some iron nanoparticles in the as-synthesized sample were coated with both gold and organic ligands instead of being completely coated with only gold. During the measurement of TGA in air atmosphere, the organics were decomposed, and the inside iron was oxidized (i.e., weight gain), which makes the absolute value of weight loss in air atmosphere be diminished.

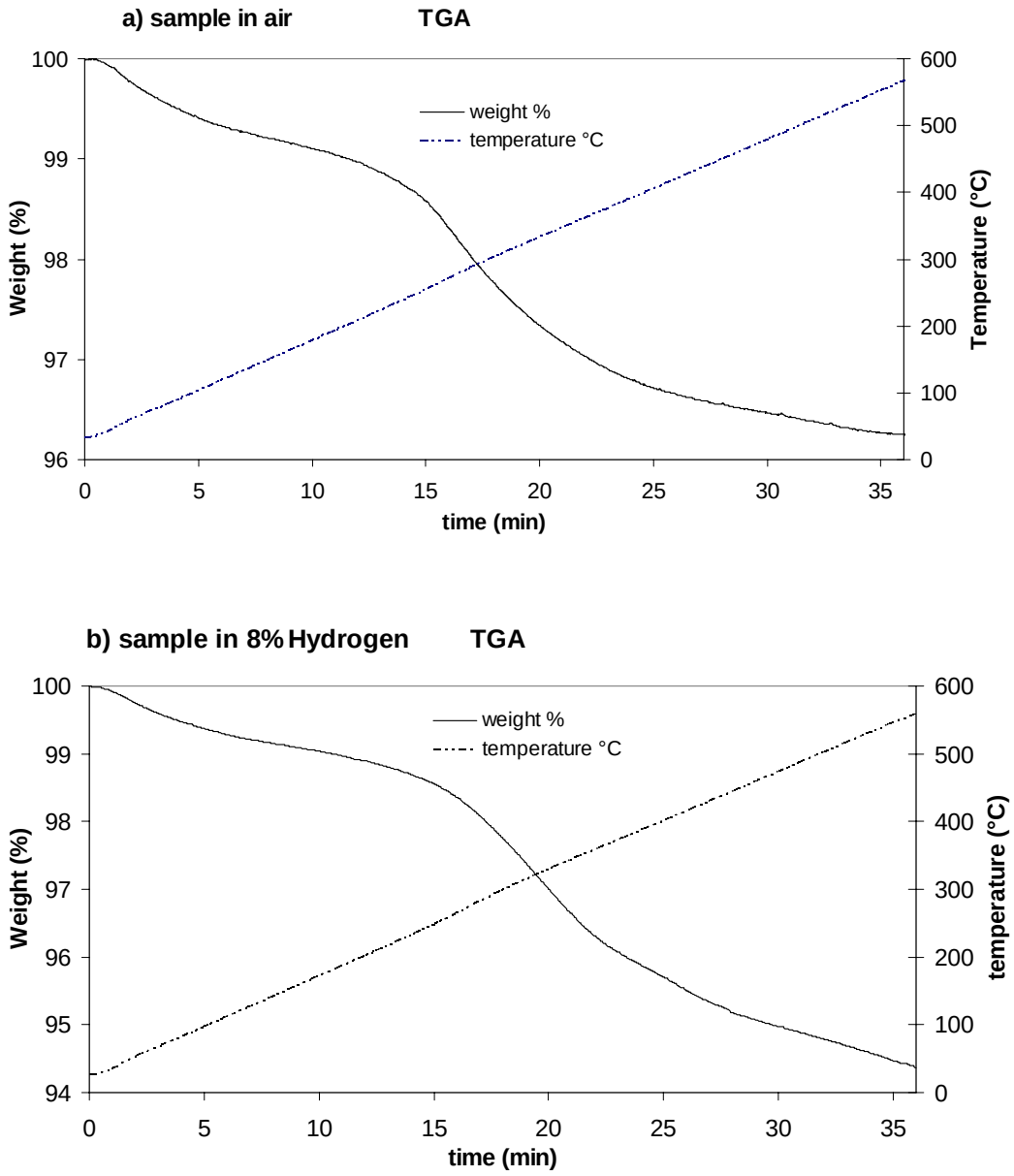

Figure 3. TGA of Fe@Au (a) in air; (b) in hydrogen.

3.3 X-ray diffraction characterization

The X-ray diffraction (XRD) pattern of Fe@Au nanoparticles is in Figure 4. All the reflections correspond to FCC bulk gold (JCPDS 4-784). The pattern of α-iron (JCPDS 6-696) is hidden under the pattern of gold due to the overlap of their diffraction peaks at 2θ=44.8°, 65.3°, and 82.5°. As shown above (Figure 1d), EDS data indicates the presence of both iron and gold. The diffraction pattern also does not show the presence of any known iron oxides. This again confirms that the iron nanoparticles are successfully coated and passivated by the gold shell.

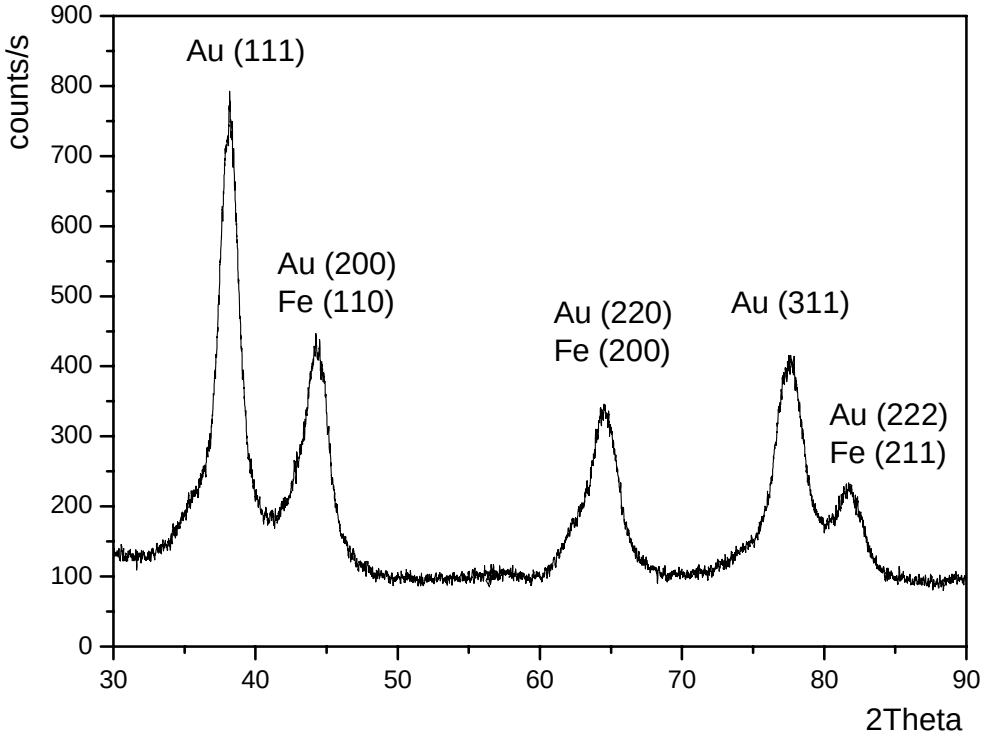

Figure 4. XRD pattern of iron coated with gold

3.4 Magnetic characterization

The Fe@Au core-shell nanoparticles are ferromagnetic at room temperature. Figure 5 shows the hysteresis loop, measured at room temperature. The core-shell particles have coercivity (H_c) of 25 Oe (see the small figure in Figure 5). The magnetic saturation is 45 emu/g. By calculation of composition from EDS and TGA data, one can estimate the value of the magnetic saturation, which is equal to 170 emu/gFe. Bulk iron has a large magnetic saturation of 216 emu/g. However, magnetic saturation of iron powders is 60-70% of that of pure iron, which is 130-151 emu/g [15]. The value that is obtained is a little higher than the value reported for iron powder. This might correspond to better crystallinity of the Fe core, as well as well passivation of its core by the gold shell. It should be mentioned that iron oxides (Fe_3O_4, γ-Fe_2O_3) are superparamagnetic in this size range, and can have a maximum magnetic saturation about 100 emu/g.

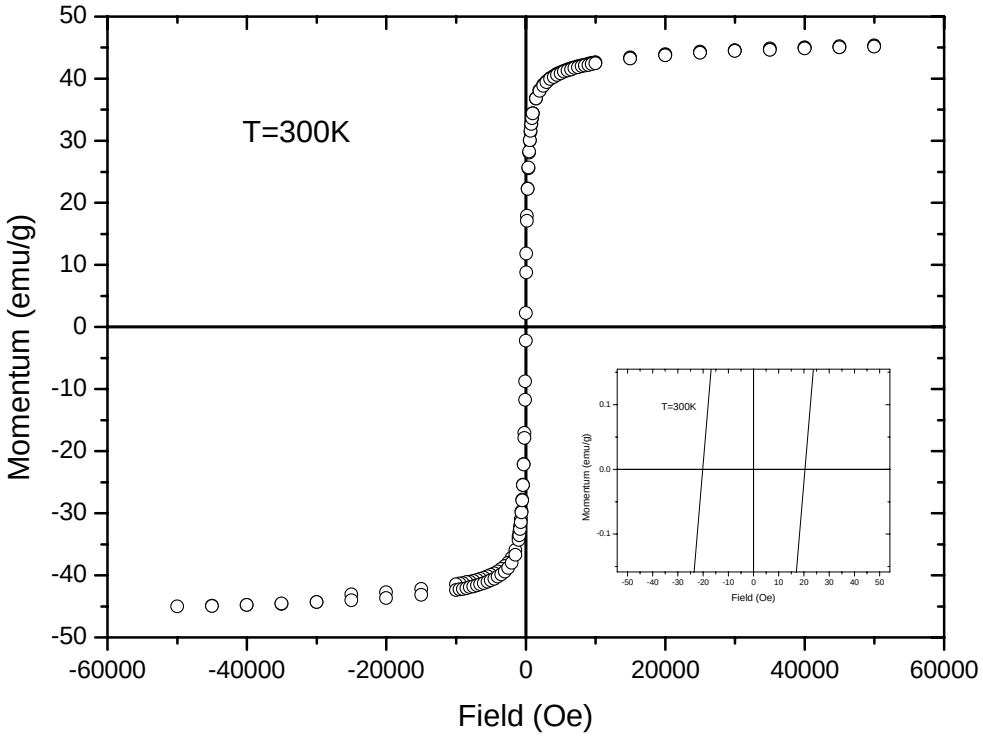

Figure 5. Magnetic hysteresis loop at room temperature for Fe@Au core-shell nanoparticles after being washed with 8% hydrochloric acid

3.5 Optical absorption characterization

It is known that pure Au nanoparticles exhibit an absorption peak due to excitation of surface plasmon (SP), i.e. collective oscillations of Drude-like conduction electrons and d-band electrons that are optically excited into the conduction band. The peak position is normally within the range of 515-530 nm and its value depends on the particle's size, shape, environment, and dielectric properties. Figure 6 shows optical absorption spectra of three samples: a –Au colloids synthesized by a two phase reaction with thiols as capping ligands, b – Fe@Au liquid phase after removal of magnetic particles (i.e., Fe@Au) from the sample, c – Fe@Au core-shell nanocomposities.

The spectrum (a) shows the SP peak at 520 nm which corresponds to isolated and randomly oriented spherical Au nanoparticles. The spectrum (b) has its SP peak at 577nm. The TEM image of this sample reveals that the majority of the sample is highly agglomerated Au nanoparticles with a size about 10 nm. A. Lazarides et al. [16] pointed out that aggregation of Au particles induces a broadening and red-shift of SP peak due to a collective interaction of the electrons of the interconnected particles.

The interesting behavior of SP is observed for the core-shell nanocomposites (figure 6c), where Au is a shell. The reported

results of the similar geometries of binary nanocomposites, like dielectric SiO_2@Au [17], semiconductor Au_2S@Au [18] and half-metal Fe_2O_3@Au [9] demonstrate that these core-shell nanoparticles have tunable plasmon resonance that depends on the ratio of the core radius to the total radius. Similarly, as in the case of Au connected particles, there is a red-shift of SP peak position with a decrease of the shell thickness and a blue-shift with an increase of the shell thickness. This effect is explained in terms of the domination of Drude-like electrons that participate in the collective plasmon resonance based on Mie scattering theory and quasi-statistic calculations. The SP peak position for our core-shell nanoparticles is centered at 680 nm. This position is relatively well matched with that reported from the calculated dependence r_1/r_2 = f (SP peak position) for dielectric and semiconductor cores, where r_1 = 5.5 nm is the core radius, and r_2 = 8 nm is the total particle radius (r_1/r_2 = 5.5/8 = 0.69). The small deviation from exact matched value r_1/r_2 = 0.75 [18], due to ferromagnetic origin of the core, which affects the dielectric properties of plasmon's environment and size deviation of shell's thickness. However, experimentally, based on our HRTEM observation with some relevant data discussed above, we would

assign this SP peak as plasmon resonance in our Fe@Au core-shell nanomaterials.

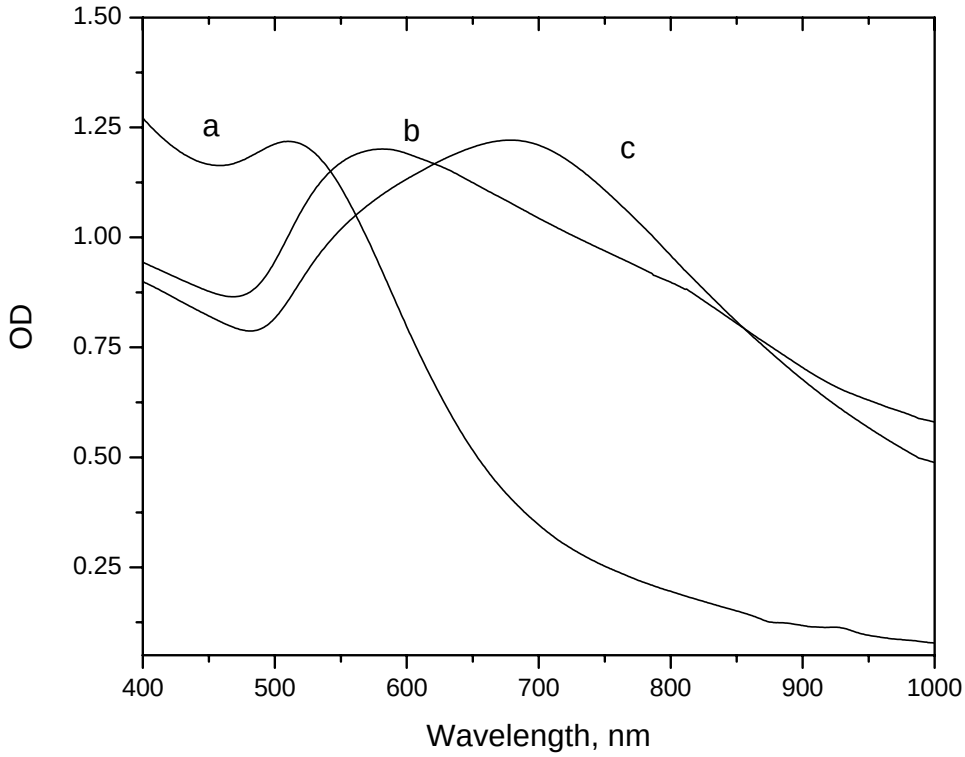

Figure 6. UV-vis spectra of Fe@Au core-shell nanoparticles.

3.6 Faraday rotation characterizations

Spectral dependence of Faraday rotation of Fe@Au core-shell nanoparticles were made in the visible range of the electromagnetic spectrum using standard normal-incidence geometry with the magnetic field parallel to the propagation of the light at room temperature. Nanoparticles were dispersed into neutral polymethylmethacrylate (PMMA) host and dried on a glass substrate. The resulting transparent magnetic film was used for the measurements. The contribution to Faraday rotation due to the nanoparticles was estimated by subtraction of the PMMA host on the glass substrate. Figure 7 shows two curves of Faraday rotation: one with a negative maximum (a) at around 460-470 nm and another one (b) at around 420-430 nm with a positive sign of rotation. The first spectrum corresponds to the rotation of plane polarized light due to Fe oxide nanoparticles (Fe_3O_4) [19] and the second one to our Fe@Au core-shell sample. The negative peak at 470 nm originates from localized states formed by interaction of 3d electrons of iron with p electrons of oxygen to give an InterValence Charge Transfer (IVCT) electron transition. Under optical excitation, electrons are transferred from Fe^{2+} to Fe^{3+} ions. This transition is mediated via oxygen; therefore, the presence of these oxidation states is required for this magneto-optical

transition to occur. Moreover, the Faraday spectrum of another magnetic γ-Fe_2O_3 does not have any features in this spectral range. Therefore our Fe@Au core-shell nanoparticles exhibit completely different behavior in Faraday rotation spectrum. The absence of iron oxide compound is manifested by the different sign of Faraday rotation and the peak position in our sample.

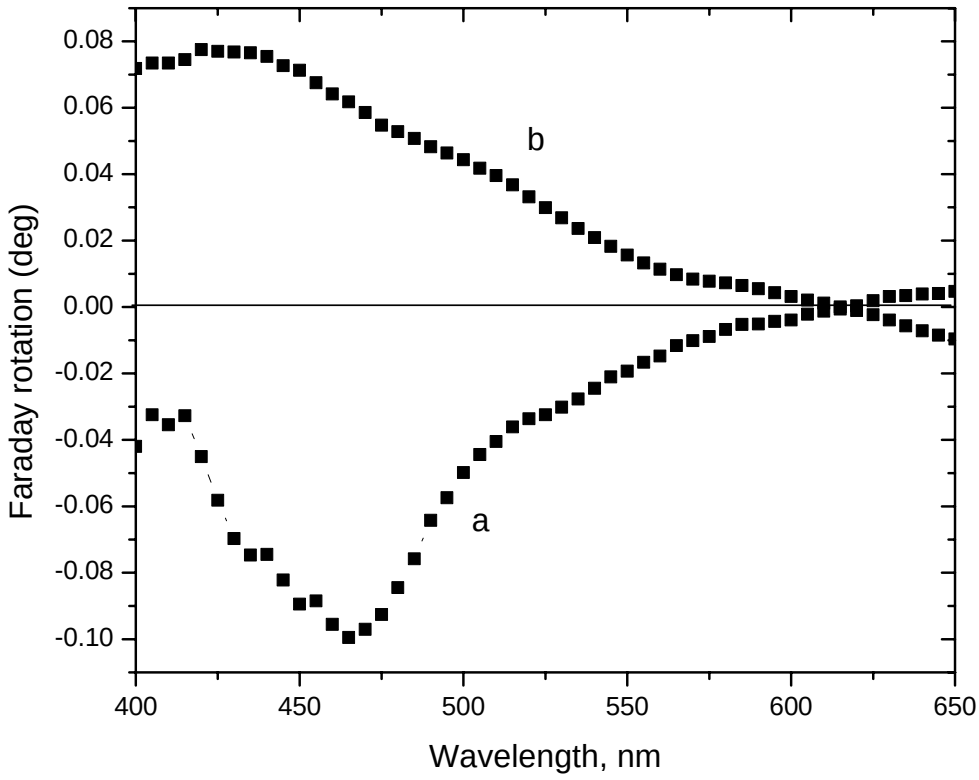

Figure 7. Faraday rotation of Fe@Au core-shell nanoparticles

CHAPTER 4 CONCLUSIONS

Gold-coated iron nanoparticles (Fe@Au) were successfully synthesized in non-aqueous 1-Methyl-2-Pyrrolidinone. Several methods were used to characterize the product. The Fe@Au nanoparticles are stable in neutral aqueous and acidic conditions, and potentially provide a wide range of opportunities for biosensor and biomedical applications. The reported method is currently being used and expanded for other systems, including the transition metals Co, Ni, Mn as a core and Pt, Au as a shell.

REFERENCES

1. F. Bodker, S. Morup, and S. Linderoth, *Phys. Rev. Lett.* 72, 282 (**1994**).
2. C. Pathmamnoharan and A. P. Philipse, *J. Colloid Interface Sci.* 205, 340 (**1998**).
3. D. V. Szabo and D. Vollath, *Adv. Mater.* 11, 1313 (**1999**).
4. E. E. Carpenter, C. T. Seip, and C. J. O'Connor, *J. Appl. Phys.* 8, 5184 (**1999**).
5. Kinoshita, T.; Seino, S.; Okitsu, K.; Nakayama, T.; Nakagawa, T.; Yamamoto, T. A., *J. Alloys and Compounds* 359(1-2), 46(**2003**) .
6. Carpenter, E. E.; Calvin, S.; Stroud, R. M.; Harris, V. G., *Chem of Mater*, 15(17), 3245 (**2003**).
7. Teng, Xiaowei; Black, Donald; Watkins, Neil J.; Gao, Yongli; Yang, Hong., *Nano Letters*, 3(2), 261(**2003**).
8. Sobal, Nelli S.; Hilgendorff, Michael; Moehwald, Helmuth; Girsig, Michael, *Nano Letters*, 2(6), 621(**2002**).
9. Lyon, Jennifer L.; Fleming, David A.; Stone, Matthew B.; Schiffer Peter; Williams, Mary Elizabeth, *Nano Letters*, 4(4), 719 (**2004**)

10. M. Brust, D. Bethell, D. J. Schi!rin, and C. J. Kiely, *Adv. Mater*. 7, 795 (**1995**).

11. Hainfeld, James F.; Powell, Richard D., *J. Histochemistry & Cytochemistry*, 48(4), 471(**2000**).

12. O'Connor, Charles J.; Carpenter, Everett E.; Sims, Jessica Ann. (USA). U.S. Pat. 2002068187

13. Kolesnichenko, Vladimir; Ban, Zhihui; Goloverda, Galina; O'Connor, Charles. Abstracts of Papers, 224th ACS National Meeting, Boston, MA, United States, August 18-22, 2002 (**2002**)

14. Sun, Yugang; Xia, Younan, *J. Am. Chem. Soc.* 126, 3892, (**2004**)

15. Asada S. *Nippon Kadaku Kaishi*, 1984, 1372 (**1984**)

16. Lazarides Anne A., Schatz George C. *J.Phys.Chem B*, 104, 460 (**2000**)

17. Averitt Richard D., Sarkar Dipankar, Halas Naomi *J. Phys. Rev. Lett.* 78, 4217 (**1997**)

18. Averitt Richard D., Westcott S. Halas Naomi J. *J. Opt. Soc. Am. B*, 16 (10), 1824 (**1999**)

19. Barnakov Yuri A., Scott Lee B., Golub Vladimir, Kelly Laurue, Reddy Ven, Stokes Kevin L. *J. Chem. Phys. Solids*, 65, 1005 (**2004**)

VITA

Zhihui Ban was born on November 5, 1972 in Yingkou, Liaoning Province, P. R. China. He earned his Bachelor of Science Degree in Chemical Engineering from Zhejiang University, which is one of the top three universities in China, in July of 1996. Then he earned his Ph. D. in Environmental Chemical Engineering from Dalian Institute of Chemical Physics, Chinese Academy of Sciences, in June of 2001. And in September of 2001, he entered the Ph. D.'s program at the University of New Orleans and joined Dr. O'Connor's group in Advanced Materials Research Institute to perform his research in nano-materials sciences. Throughout most of his academic career in University of New Orleans, he worked in a laboratory at AMRI as a research assistant. In the spring of 2004, Zhihui received his Master of Science degree.